International Journal of Innovative Research in Advanced Engineering (IJIRAE) ISSN: 2349-2163
Issue 06, Volume 6 (June 2019) - Special Issue www.ijirae.com
SPECIAL ISSUE - 4th National Conference - "RTME – 2019"

INVESTIGATION OF STRUCTURAL INTEGRITY IN INTEGRATED BLADED ROTOR (IBR) OF A GAS TURBINE ROTOR

Dr. Kumar Kenche Gowda
Vivekananda Institute of Technology, Bengaluru, Karnataka, India
Dr. AJIT PRASAD
PES College of Engineering, Mandya, Karnataka, India
Dr.Ramachandra K
RV college of Engineering, Bengaluru Karnataka ,India

Manuscript History
Number: **IJIRAE/RS/Vol.06/Issue06/Special Issue/SI.JNAE10088**
Received: 28, May 2019
Final Correction: 05, June 2019
Final Accepted: 10, June 2019
Published: **June 2019**
Editor: Dr.A.Arul L.S, Chief Editor, IJIRAE, AM Publications, India

Abstract: A heavy duty gas turbine rotor operates in a highly nonlinear environment. It is often taken to thermal transients and over-speed events. The source of excitations often excites the blades during in-service life. Various stresses generated in the turbine rotor are not only due to centrifugal forces but also due to wake forces generated during the flow through airfoil, which later generates fatigue, Vibratory and creep loads. Structural failures may occur due to various uncertainties involved in the operation of gas turbines such as speed loads, over-speeding and component manufacturing deviations. If catastrophic rotor failures occur, they commonly result in lengthy forced outages and severe economic penalties to the affected utilities. In the present work, assessment of structural integrity of Integrated bladed rotor assessment is accomplished through conduction of an Finite Element analysis blended with classical theories. The structural analysis results of IBR is compared with Bladed Disc assembly to highlight the effect of Contact at Blade Butting zone on frequency response along with Integrated Model(IBR) for a given flow conditions and airfoil. In addition to evaluation of structural strength in the rotor disc components, failures due to vibrations are also quite apparent in the Gas turbine blades. An attempt is made to investigate the resonance points at operating speeds, disk mode participations if any and retrieve excitation frequency modes, Campbell, SAFE (Singh's Advanced Frequency Evaluation Diagram) are generated and analyzed to evaluate the separation margins for Blade and disk integrity.

Keywords: Circumferential entry blade, Axial entry blade, Spacer, Campbell diagram, High cycle fatigue, Stage efficiency, Mechanical integrity.

I. INTRODUCTION

Structural integrity of Gas turbines plays an important role in providing better service life to the engine. The gas engine rotor blade is the heart of the engine. Providing Mechanical Integrity .is the most challenging task in rotating machines due to their frequent failures. However, the modern manufacturing techniques have shoulder the possibility of generating IBR's Integrated bladed rotors, followed by the design office verification, promising the reliability and robustness in the design [1]. Blade deteriorations, distortions due to unsteady flow, surge, stall leading to notable reduction in the gas-turbine's performance [2]. Gas turbine manufacturers are constantly focusing on improving the design to produce more efficient, high thrust and light engines. Axial flow compressors form the initials stages with low, intermediate and finally high pressure stages are important. Each stage of compressor consists of series of rotating blades followed by stationary blades.

The design of turbo machine blade is of a great challenge. Integrity has to be achieved in both aerodynamic and mechanical against stringent design checks. To achieve these goals, improvement in compressor rotor blade design is very essential. Theories from notable literature, explains the behavior of regenerative machines namely: momentum exchange theory, shear stress theory, theory of air-foil blading, and compressible flow theory [6]. Senoo [7] compared the momentum exchange theory with the shear stress theory and concluded that the two approaches were compatible with physics of the problem. In the following years, different researchers like Meakhail et al. [8] accredited the momentum exchange theory as the most correct. Most previous researchers used mathematical models based on exchange theory and adopt one inlet angle and one exit angle. Due to the variations in geometry, Meakhail and Park [5] proposed another mathematical model for turbo-machines based on momentum exchange theory and adopt one inlet angle and two exit angles. This model showed some discrepancy with experimental data when applying it on the turbo-machines.

The effect of blade numbers on the turbo-machine performance was investigated by Iversen et al. [9], Badami [10] and Grabow [11]. Choon and Jang [12] studied the influence of blade number and extension angle on the performance. They concluded that increasing of blade numbers leads to increase of the pressure and improves the efficiency. These previous works didn't include the study of effect of blades number by using CFD technique. This work was carried out by T.Mekhail [4] by investigating the performance; in addition to mathematical model based on momentum exchange theory and these results were also validated experimentally. By utilizing the above mentioned literatures effectively the study of performance is carried out. In the present work agas engine compressor rotor blade disk and Blisk is checked for resonance at design stage for vibrations at off-design conditions. Flutter in aero engines has been one of the causes for introducing fatigue failure of its components. It is due to the unbalanced exchange of energy between flowing air and the vibrating structural component (The component tends to extract more energy from the air flow than it can dissipate). The axial flow compressor is a candidate component for a wide variety of aero engines because of their light weight, smaller volume and also for possessing a simple mechanism for air flow path. It does work on gas passing through it while raising its pressure and enthalpy. An axial flow compressor contains several stages, with each stage comprising a rotor or disk which is mounted on a central shaft and rotating at high speeds, together with the stator fixed to the casing. Both rotor and the stator have many aerodynamic profile blades designed to generate a pressure difference across the stage. The components of a gas turbine engine are exposed to vibration caused by unsteady forces resulting from relative motion between rotating and non-rotating parts. These vibrations have been catastrophic and these aspects have been well researched by many investigators [38], [39], [86] in several perspectives.

The flutter or self-excited vibrations of aero engines can be best analyzed through numerical simulation methods [49]. The bladed disk assembly and blisk considered in this investigation has been analyzed for these aspects by loading them on similar lines encountered in actual practice and as recommended by earlier investigations as well [49]. The results of symmetric modal analysis of the model considered in this investigation have been examined through Interference and Campbell diagrams, specifically developed for the purpose.

NOMENCLATURE

- API – American Petroleum Institute (Standard 616)
- α_1, α_2 – Inlet velocity angles
- β_2, β_1 – Outlet velocity angles
- V_1, V_{r2}, V_{r1}, V_2 and U – Respected Inlet and outlet velocity
- E - Energy input per stage (unit mass flow)
- W- Work done (unit mass flow)
- η_S– Stage efficiency
- η_b– Blade efficiency
- η_N– Nozzle efficiency(.98)
- ρ- Velocity ratio

OBJECTIVES

The bladed disk assembly and blisk considered in this investigation has been analyzed for these aspects by loading them on similar lines encountered in actual practice and as recommended by earlier investigations as well. The analyses include estimation of diametric mode shapes of bladed disk assembly and blisk by invoking the principles of cyclic symmetry and consideration of stress stiffening & spin softening effects when subjected to centrifugal loading. The following areas of interest are focused in the present work

- Achieve Mechanical Integration in airfoil design with an ideal smooth transition radius to minimize the localized stresses at blade hub [1]

- Analyze the blades frequency separation margins
- Achieve a customized methodology for frequency evaluation in compressor rotor blade design
- Study the influence of number of blades and mechanical efficiency of the turbine
- Conduct vibratory analysis to investigate resonant frequency and separation margins
- High cycle fatigue evaluation to investigate maximum endurance stress for each design case and estimate the number of life cycles.

DESIGN SPECIFICATIONS

The following specifications are considered for analysis and calculations of stage efficiency.

- Rated speed: 16000 RPM
- Material of blade and locking pins: Ti-6Al-4V
- Material of the disc: Inconel 718.
- Over-speed condition: 121% as per API 616 standards.

SIMULATION METHODOLOGY

A geometric model consisting of bladed disc, optimized blisk is taken into consideration for a non-linear pre-stressed modal analysis. The base line model and topologically optimized blisk is illustrated in figure 2. It is important to note that the airfoil of bladed disk and blisk are the identical. The location, number of blades, disk dimensions radially along with Aft end. Considering the arrangement of the blades on the rim of the compressor, cyclic symmetry of the blade and disk assembly and blisk has been invoked during the analysis of different parameters contributing to their failure during their in-service conditions carried out in this investigation. Accordingly, a sector of both blade and disk assembly and blisk has been considered for analysis in this work. Since cyclic symmetry has been assumed, constraints have been provided in the axial and tangential directions while no constraints are included in the radial direction, which is in agreement with the similar type of investigative analysis carried out on 2D models of rotating components by earlier researchers . Similarly, the requisite constraints have been assumed in the axial direction when one sector of bladed disk assembly is in axial contact with the other, while constraints have been invoked in the tangential direction on the front end of the assembly as per the requirements of the analysis. An FE analysis is conducted for the above mentioned cases to stringently compare structural integrity, for vibration characteristics for the best design condition.

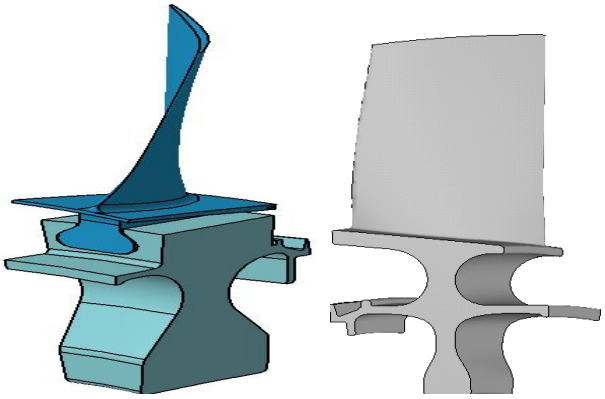

Fig. 1: Base line geometry and optimized blisk for evaluation

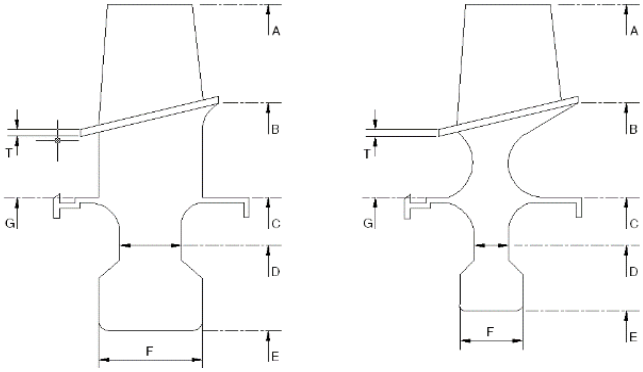

A: Blade height D: Web thickness T: Platform thickness
B: Outer disk radius,E: Bore radius,C: Bolt end radius, F: Bore thickness
Fig.2: Topological comparison of two dimensional bladed disk and proposed blisk

DESIGN CONSIDERATIONS FOR ACHIEVING MECHANICAL INTEGRITY

To achieve the objectives, the following assumptions are considered: Working fluid considered is air with mass flow rate of air as 20 kg/sec, inlet pressure is 1.01325 bar, inlet temperature is 301 K, Tip Speed is 350 m/s, Axial velocity Ca is 150 m/s and stage efficiency is 90.45% [2,3]. Pressure ratio is 4.15 and hub diameter is 278 mm [3]. Number of stator blades is 33 and Number of rotor blades is 40. Blade transition radius of 2mm and angle of attack is 18°. Factor of safety assumed is 1.68 for allowable gross yield stress of 357.7689 MPa. High aspect ratio blade of 2.25 aspect ratio with a blade height is 81mm and chord length of airfoil is 36 mm. Over-speed rotor blade testing speed is assumed as 121% as per American Petroleum Institute (API) standards.

The blade material chosen is Titanium alloy (Ti-6Al-4V) and properties are shown in Table 1.

Table 1. Ti-6Al-4V mechanical properties

Specific properties at 316° C							
Density (1000kg/m^3)				4.28			
Elastic Modulus (GPa)				110			
Poisson's ratio				0.33			
Tensile strength(MPa)				993			
Yield strength (MPa)				930			
Percent elongation (%)				14			
Composition	Al	V	C	Fe	N_2	O_2	Ti
Weight %	6.0	4.0	0.8	0.2519	0.05	0.2	Remainder

PERFORMANCE OF TURBINE

In the present work an air-foil of the blade remains same for both bladed disk and blisk. The structural integrity achieved by the enhanced disk dimensions for weight reduction and disk mode participation during the in-service condition. typical velocity diagram considered for the analysis is shown in Figure3.

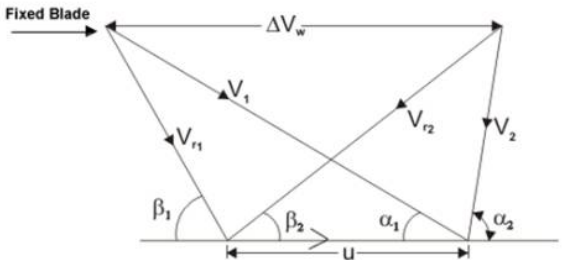

Fig.3: A typical velocity diagram for the compressor stage

The velocity triangles are symmetrical,

$\alpha_1=\alpha_2$; $\beta_1=\beta_2$,$V_1=V_{r2}$; $V_{r1}=V_2$

Energy input per stage (unit mass flow)

$E=\frac{V_1^2}{2}+\frac{V_{r2}^2-V_{r1}^2}{2}$, $E=V_1^2-\frac{V_{r1}^2}{2}$

The above equation can be written as,

$E=V_1^2-\frac{V_1^2}{2}-\frac{U^2}{2}+\frac{2V_1UCos\alpha_1}{2}$

$E=(V_1^2-U^2+2V_1UCos\alpha_1)/2$

From inlet velocity triangle,

$V_{r1}^2=V_1^2-U^2+2V_1UCos\alpha_1$

Therefore the work done (for unit mass flow rate) is given by,

$W=U\Delta V_W=U(2V_1Cos\alpha_1-U)$

The blade efficiency,

$$\eta_b=\frac{2U(2V_1Cos\alpha_1-U)}{V_1^2-U^2+2V_1UCos\alpha_1}$$

By substitution,

$$\rho=\frac{U}{V1}\quad,\eta_b=\frac{2\rho(2V_1Cos\alpha_1-\rho)}{1-\rho^2+2\rho Cos\alpha_1}$$

For present work the blade efficiency is assumed to be maximum by considering ideal conditions.

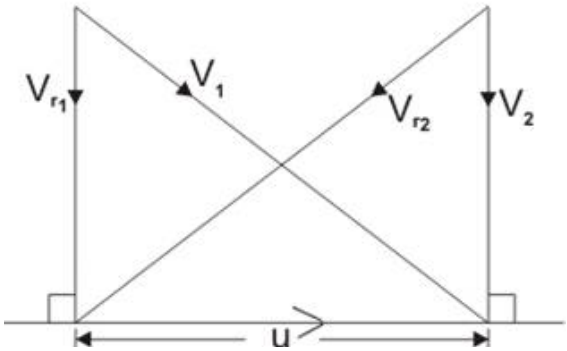

Fig.4: Velocity diagram for maximum efficiency.

The energy transfer in this case,
$E = U\Delta V_W = U^2$,The blade efficiency can obtained from,

$$(\eta_b)_{max} = \frac{2Cos^2\alpha_1}{1 + Cos^2\alpha_1}$$

Turbine stage efficiency is equal to product of blade efficiency and nozzle efficiency
$\eta_S = \eta_b * \eta_N$, $\eta_S = 88.78\%$

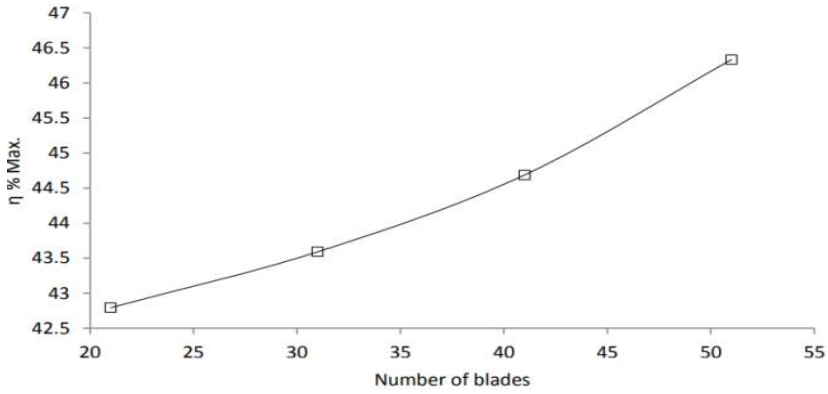

Fig. 5: Maximum efficiency at different number of blades [4]

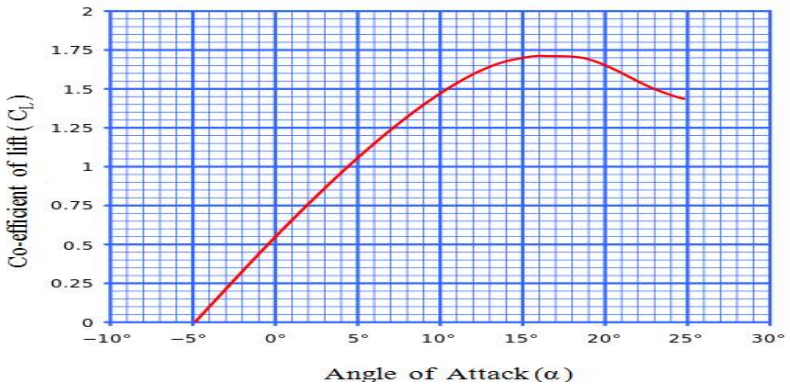

Fig.6. Co-efficient of lift (CL) v/s Angle of Attack (α)[13]

Figure 2 shows that for 16° to 18° angle of attack, maximum lift co-efficient is obtained, which is 1.70.
Exit static pressure is applied as the exit boundary condition. Speed of 16000 rpm is applied as the rotational speed for the rotor with a hub-tip ratio of 0.475 for the present research work. Figure 6 shows variation of Hub-Tip Ratio v/s Speed in rpm of the compressor rotor. Periodic Steady state analysis is performed with stage interface applied between the stationary and rotating components. Shear Stress Transport (SST) turbulence model is considered for this Computational Fluid Dynamic analysis and the blade is staggered from 2° to 18° to get the ideal flow over an airfoil.

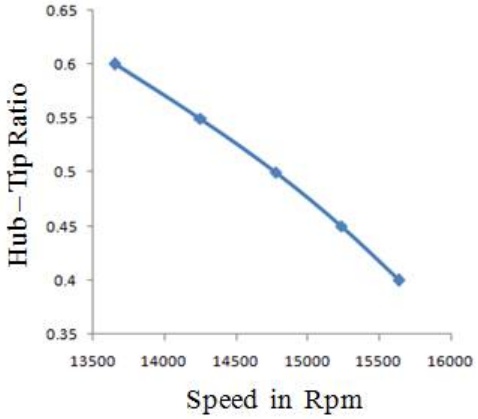

Fig. 7. Variation of rotor blade Hub – Tip Ratio

VIBRATION ANALYSIS OF BLADED DISK AND BLISK

Transient stresses are attributable to several sources but are primarily due to blade excitation at a frequency equal to the natural frequency of the blade. Transient stresses are more rigorously defined as alternating, cyclic, or vibratory stresses.

Steady state stresses are routinely calculated at critical points on the blade by using principles of the mechanics of deformable bodies and mechanical systems design. Frequency evaluation in cyclic symmetric structures using finite element analysis is through modal analysis. The approach is as follows:

- All analysis is based on single-blade cyclic sector. Assuming all blades are identical.
- Pre stressed Modal (frequency) analysis is based on simulation of full bladed disk frequency and mode shape analysis through modal cyclic symmetry analysis.
- Frequency predictions to be performed for a number of different nodal-diameter
- Frequency prediction includes stress-stiffening (increases the frequency) and spin-softening (decreases the frequency) effects.
- Temperature of 300 ^{o}C (572 F) is assumed for the stage.
- Full Contact is assumed for butting faces between blade and disk. For a full contact condition, the interface is assumed to have "no slip" condition for the entire pitch and all blades are assumed to be identical.
- Separation margin at operating speed is considered to be of operating speed at design point.

Turbo-machinery components are subjected to widespread excitations due to gas loads. Such powerful excitations may cause resonance in the rotating structure which leads to decreased structural performance. Therefore conduction of a vibration analysis using a Campbell diagram is highly encouraged (Industry best practice). Separation margins of 5% is considered for an operating speed of 16000 RPM i.e. a left margin of 95% and a right margin of 105% is considered along with a generous margin of 121% on the right side as per API standards (off design over-speed condition). Six excitation frequencies are considered to ascertain there are no resonances present in the separation margin as specified.

NUMERICAL INVESTIGATION AND RESULTS

Geometrically modeled and meshed, bladed disk as explained earlier is used for the vibration analysis. Only first six fundamental mode shapes are evaluated [38] corresponding to 20ND (nodal diameters) by considering centrifugal and thermal loads to include the pre-stress effects. The mode shapes obtained are graphical representation of possible eigen vectors of the blades in a bladed disk assembly as shown in Fig 10.

In order to examine the interference of the blade natural frequency with the exciter frequency, Campbell diagrams have been developed as per the procedure available in the published literature [39]. Campbell diagram establishes the relationship between the rotating speeds of the components of an aero engine with its frequency of vibration for different exciters (engine orders), which are calculated as the excitations caused per revolution of the disk on each blade. 20 such engine orders have been considered to cover the entire range of the first 6 fundamental modes while the engine rotates at a speed of 16000rpm. Resonance occurs when the frequency of a particular mode shape is in the close vicinity of the engine order frequency in the operating speed regimes of the components. Frequencies obtained at different speeds are tabulated in Table 5.1 to draw the Campbell diagram for critical nodal diameter ND = 6. It is evident that the stress stiffening effect has increased the stiffness of the assembly and the frequency increases linearly with the engine speed.

Table: 2 Natural frequencies of bladed disk assembly

Speed	Mode1	Mode2	Mode3	Mode4	Mode5	Mode6
0	520	1291	1984	2714	3370	4078
16000	737	1615	2357	3201	3843	4536
17000	739	1630	2397	3230	3879	4565

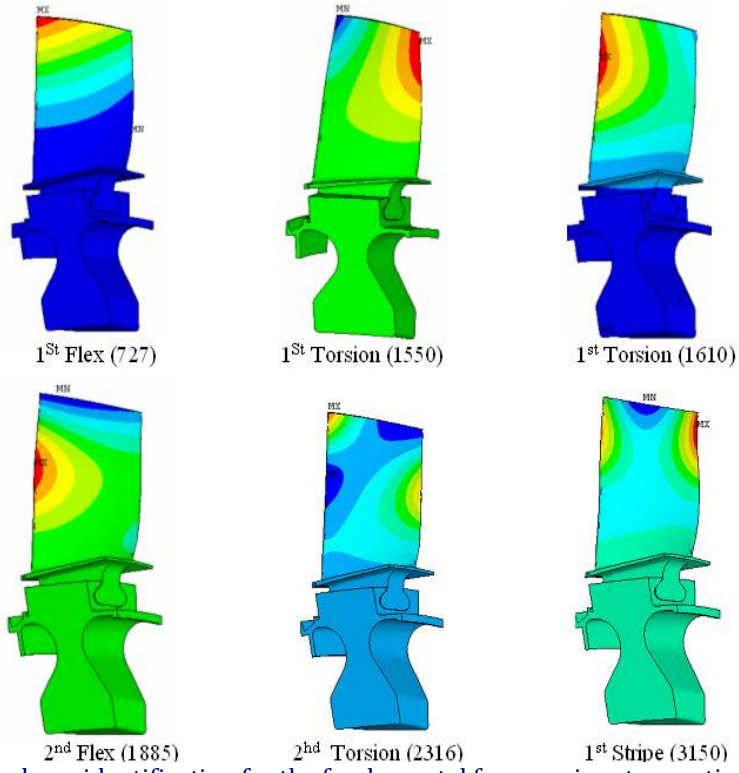

Fig.8:Mode shape identification for the fundamental frequencies at operating speed

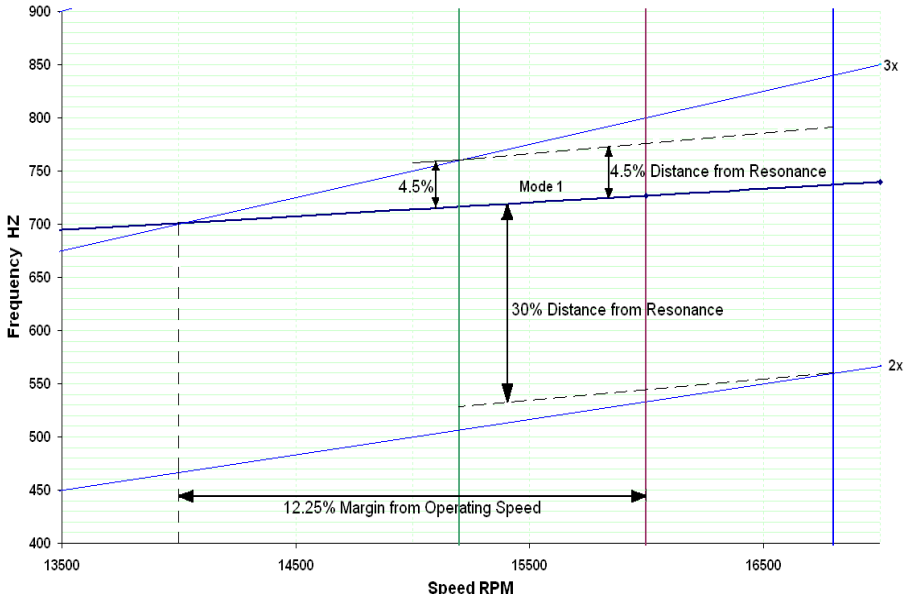

Fig 9: Speed and frequency margins for first mode from 2X and 3X excitations

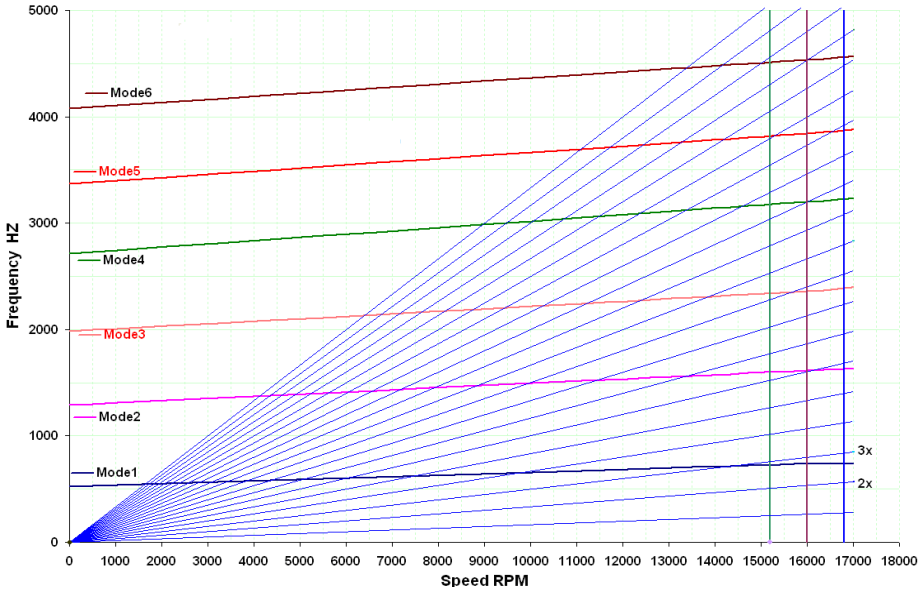

Fig 10: Campbell diagram for bladed disk at 121% speed

Campbell Diagram: Observations

- Frequency predictions show that the fundamental cantilever mode is placed between 2 and 3 per-rev excitation as shown in Fig10
- Predicted separation margin for this fundamental cantilever mode is at least 12.25% to the left of operating speed as shown in Fig 9
- The cantilever mode has an upper bound margin of 4.5% and lower margin of 30% in the exciter box, which qualifies the blade at design point.
- Mode 2 is having crossing over at operating speed range at 6 per /rev excitation.
- Observations show that modes in families higher than the first mode family can have low speed margins and hence can be almost resonant.
- Harmonic response analyses need to be performed to assess resonant stress amplitudes for these modes, to evaluate the HCF margins at critical zones.

SAFE diagram: Bladed disk

In a bladed disk structure, the fundamental natural modes of vibration can be categorized as cantilever, tangential, axial, or torsion. Associated with each of these fundamental mode families, are a series of 'nodal diameter' or 'disk effect' [40] modes. When one of these modes is excited, the amplitude of vibration can vary harmonically around the disk and the phase relationship between substructures shall also change. The number of complete sinusoids around the disk (nodal diameter number) is used to describe the mode.

It should be noted that the natural frequency would vary with nodal diameter for short blade length. Consider a case of 40 blades around the circumference and having nodal diameter range from 0, 1, 2…20. Natural frequencies have been extracted for 40 blades. First 6 fundamental modes are extracted using Lanczos algorithm employed in ANSYS. The modes as indicated are mode shapes of individual sectors and nodal diameter is one which indicates the vibration mode of disk.

Physical understanding of interference diagram is risk evaluation due to resonance. The following important points are to be noted while studying an interference diagram:

- There exists no general rule for change in natural frequency with respect to nodal diameters. In the present case, an increase in natural frequency with increase in nodal diameter is observed.This may be due to the fact that the system becomes stiffer at higher modes and nodal diameter is nothing but disk mode.
- Some researchers have observed that shrouded assembly is more sensitive to nodal diameters than unshrouded assemblies. But strictly speaking there is no defined pattern of natural frequency variation with respect to nodal diameters.
- Among all possible nodal diameters, it is possible to single out a few which will cause maximal damage to the system i.e. pump in max energy into the system. These nodal diameters are referred to as critical nodal diameters. Total no of vanes for this stage is 34, for 40 numbers of moving blades and 34 stator blades, nodal diameter 6 i.e. (40-34) becomes highly critical .

Plotting SAFE diagram

Figure11: shows a typical SAFE diagram with points representing nodal diameter modes belonging to one fundamental mode family. The number of nodal diameters are plotted along X-axis while, natural frequencies of fundamental mode families are plotted along Y-axis.

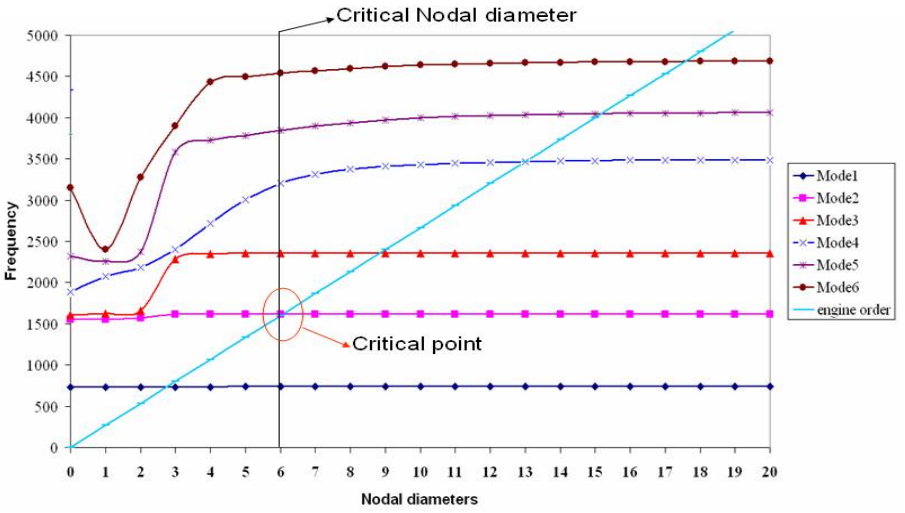

Fig 11: SAFE diagram for bladed disk

The interference diagram co-relates nodal diameters with that of vibrating frequencies not only to identify the pattern of mode shapes but also to examine the influence of disk contributions to vibrations of assembly. A typical list of natural frequencies thus obtained from a cyclic symmetric modal analysis at different nodal diameters as shown in Table3. For 34 vanes the vane passing frequency (VPF) is 9066Hz. This frequency occurs faraway from first six fundamental mode families under consideration

Table:3: Frequencies of the first 6 modes at different nodal diameter

Nodal Dia	Mode1	Mode2	Mode3	Mode4	Mode5	Mode6
0	727	1550	1610	1885	2316	3150
1	729	1555	1628	2078	2255	2404
2	731	1573	1659	2188	2375	3272
3	734	1613	2285	2399	3587	3903
4	735	1614	2349	2713	3730	4431
5	736	1615	2355	3007	3785	4493
6	737	1615	2357	3201	3843	4536
7	738	1616	2358	3312	3896	4571
8	738	1616	2359	3374	3938	4598
9	738	1616	2359	3411	3971	4619
10	738	1616	2359	3434	3995	4635
11	738	1616	2359	3449	4012	4648
12	738	1616	2358	3460	4025	4657
13	738	1616	2359	3467	4035	4664
14	738	1616	2359	3473	4042	4670
15	738	1616	2359	3477	4047	4674
16	738	1616	2359	3480	4051	4677
17	738	1616	2359	3483	4054	4679
18	738	1616	2359	3484	4056	4680
19	738	1616	2359	3485	4057	4681
20	738	1616	2359	3485	4057	4681

Observations: SAFE diagram

It is clearly evident from the above results that natural frequency depends to a considerable extent on nodal diameter (Disk modes).

- Doublets in natural frequencies are observed for all nodal diameters except ND =0. These modes occur either as double modes (Two modes have identical frequencies and similar mode shapes) or single modes and can be defined by and as sinusoidal variations of circumferential displacements around the bladed disk. A double mode is defined by variations of the circumferential displacement where sinusoidal order 'n' is the number of lines of zero displacement across the assembly or, as is generally known, the number of nodal diameters and 'θ'is the angular separation of two adjacent blades.
- The cantilever mode has no crossing over due to running speed harmonics at operating speed.
- Running speed harmonics line crossing second mode family indicates resonance at critical nodal diameter ND 6, which calls for estimation of resonant vibratory stresses.

The name "Interference Diagram" itself arises from the occurrence of "Interference" at critical nodal diameters. The main edge, interference diagram possesses over other diagrams like Campbell diagram is due to the critical nodal diameters. Critical nodal diameters represent the interference of two waves i.e. running speed harmonic wave and vane passing frequency harmonic wave. From elementary physics, interference occurs when two waves with same frequency are in phase, the waves add up and produce a net wave, which has amplitude equal to the summation of amplitudes of both the waves.

Harmonic response and HCF analysis of bladed disk

Any sustained cyclic load will produce a continuous cyclic response (A harmonic response) in a structural system. Harmonic response analysis enables the prediction of sustained dynamic behavior of the structures, thus facilitating verification of design with respect to overcoming resonance, high cycle fatigue and other harmful effects of forced vibrations. Harmonic response analysis is a technique to determine the steady-state response of a linear structure subjected to loads that vary sinusoid ally (Harmonic) with time. The methodology is to calculate the structure's response at critical frequencies and obtain a relationship of some response quantity (Usually displacements) as a function of frequency. "Peak" responses are then identified on the plot and stresses reviewed at those peak frequencies. This type of analysis technique calculates only the steady-state, forced vibrations of a structure. It is seen from Campbell diagram obtained for bladed disk assembly, that mode families higher than the first mode family have low speed margins and hence can be almost resonant. A harmonic response analysis is performed to assess resonant vibratory stress amplitudes for these higher modeswith following assumptions.

- Mode is resonant with corresponding per-rev excitation.
- Modal damping ratio for each of the modes of interest is 0.002 or 0.2% (Damping ratio with respect to critical damping).
- As a common basis, a stimulus (Gas loads) of 5% is applied on airfoil surface [49]. The magnitude of vibratory forcing is 5% of the steady forcing. In reality, the stimulus may range from 1 to 5% for lower harmonics (per-rev).
- Forced harmonic analysis, is employed with worst possible scenario of gas loads Stimulus) at critical resonance points to estimate the alternating vibratory stresses. These are imposed on Goodman diagram, to obtain the vibratory margins available at resonant modes for the predictions of HCF life margin, for the given material and temperature with a factor of safety of 1.3 on ultimate and endurance stress limit for $1e^7$ cycles as safe limit.

The above mentioned procedure has been used to evaluate harmonic response of the bladed disk assembly. Fig 5.6 shows the amplitude response of blade airfoil for 5% stimulus

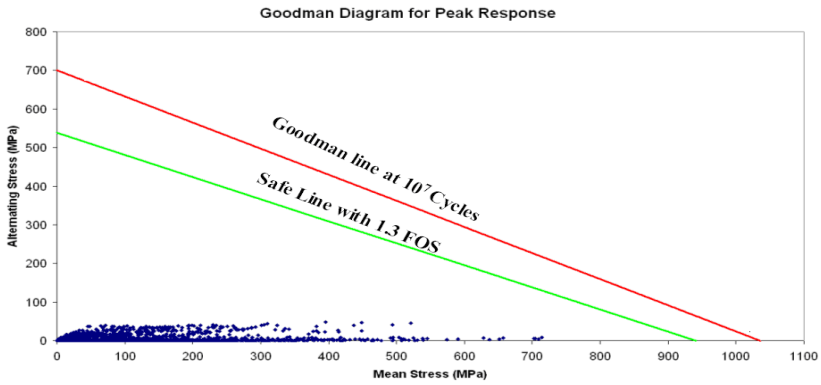

Fig 12: Goodman diagram for evaluation of vibratory stress margin

Maximum amplitude of the vibration is found at 750 Hz which is close to the first natural frequency of bladed disk assembly. Subsequent peaks are found at other natural frequencies of the assembly. The stress evaluation has been carried out at amplitudes varying from maximum to minimum. Maximum peak stress is found to be 47 MPa for mode two frequencies. The stresses obtained from harmonic analysis is then used with static stress analysis to plot Goodman diagram for mode 2 (Fig12) which shows reasonable margin of safety for alternating stress thus indicating longer life of the component even at resonance condition. For a mean stress of 790 MPa (Static analysis) allowable alternating stress from Good man diagram is 110MPa at a Factor of safety line. From Goodman diagram it appears that a peak alternating stress of 47 MPa can sustain 107 cycles at resonant frequency.

Frequency evaluation of blisk

Employing similar principles and operating conditions of bladed disk cyclic symmetry modal analysis of blisk configuration is carried out to evaluate the frequency margins. The analysis is repeated at various speeds to compute the blade frequency at operating conditions. Resulting frequencies are tabulated in Table 4. The fundamental mode shapes of blisk at design speed are as shown in Fig 13. Mode identification is very important in judging the behavior of blade at critical locations. the frequencies are scattered on a Campbell diagram as shown in Fig 13.

Table: 4 Natural frequencies of bladed disk assembly

Speed	Mode1	Mode2	Mode3	Mode4	Mode5	Mode6
0	720	1800	2340	2960	4640	5760
16000	888	2222	2689	3291.6	5675.9	6765.9
17000	900	2260	2713	3310	5760	6830

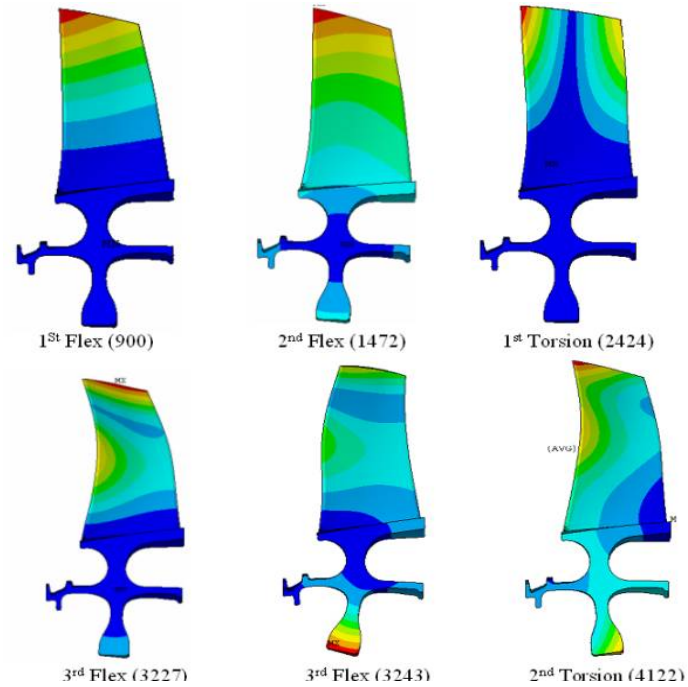

Fig.13: Mode shape identification for Blisk fundamental frequencies at operating speed

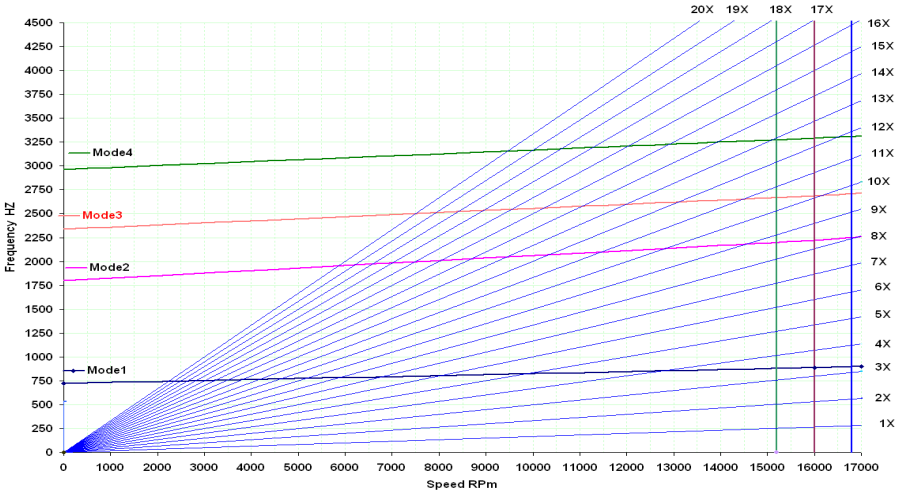

Fig 14: SAFE diagram for bladed disk

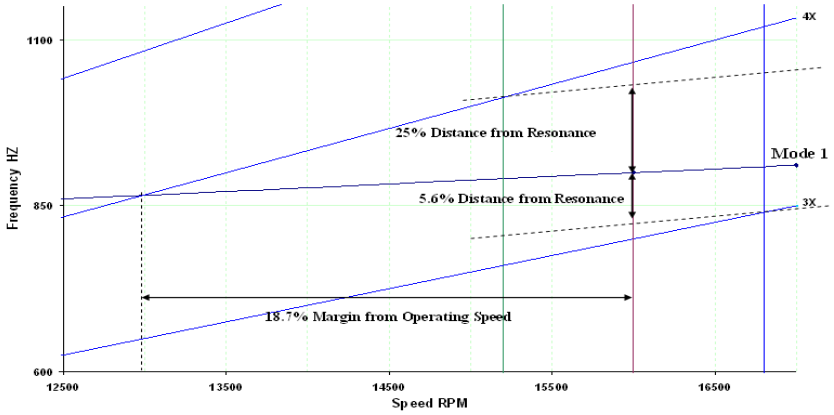

Fig 15: Speed and frequency margins for first mode from 3X and 4X excitations

In case of blisk, all the modes are spread across evenly and are quite far away from the exciter box and hence blisk has very less chances of resonance which is considered to be safe from the view point of HCF margin. The disk participation is more due to thinning of blisk.

Campbell diagram: Observations

- Frequency observations indicates the fundamental cantilever mode is placed between 3 and 4 per/rev.
- Higher frequency values have been reported for blisk configuration due to integration of blade and disk components with reduced mass.
- Predicted speed margin for this fundamental cantilever mode is at least 18.7%.to the left of the operating speed for 4 per/rev excitation.
- The cantilever mode has an upper bound margin of 25% and lower margin of 5.6% in the exciter box, which qualifies the blade for design point.
- Third mode has a crossing over at operating speed range at 10 per /rev excitation.
- Predictions show that mode families higher than the first mode family have low speed margins or in almost resonant from Campbell diagram.
- Harmonic response analysis is performed to assess resonant stress at this critical point.
- The vane passing frequency value is 9066 Hz for given 34 vanes. It does not affect any of the higher modes under consideration.

SAFE diagram for Blisk(IBR)

Fundamental frequencies for first six mode families are computed up to 20 ND for blisk configuration. The frequency data is represented in table 5. The frequency scatter at design speed is indicated on a interference diagram as shown in Fig 16. With increase in nodal diameters the frequencies of fundamental mode families stabilize at higher nodal diameters at operating speed. The absence of blade and disk contact (Friction), reduction in stage mass due to topological optimization, has resulted in higher frequency mode families compared to bladed disk assembly (Ref Fig 16). These, modes are to be checked for interference possibilities with NPF at 9066 Hz.

Thin disk of blisk has introduced disk mode interference between the fundamental mode families. For instance, mode 3 and mode 4 appears closer, with less frequency margin at ND 2, which can be noticed from interference diagram. Similarly, mode 2 appears closer and mode 3 at ND 5. Such possible modes are called (complex modes). Appearance of these modes at critical nodal diameters may result in high potential resonance, leading to HCF failures. There is no critical mode in case of blisk, compared to bladed disk, where 2nd mode is found critical at nodal diameter 6.

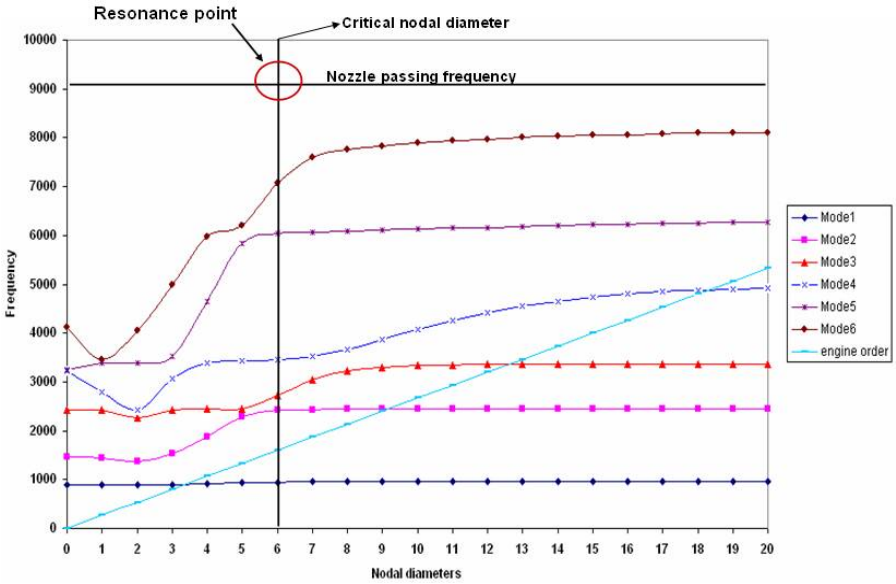

Fig16: SAFE diagram for blisk

Observations: SAFE diagram

The cantilever mode lies between 3 and 4 per /rev excitation with no crossing over from running speed harmonics at operating speed as shown in Fig16.

Observations show that mode families higher than first mode family have low speed margins and hence can be almost resonant.

Interference diagram clears the possibility of changing vane count, due to blade vane interaction at design speed

HCF analysis of IBR

Procedure similar to that followed in case of bladed disk has been followed to evaluate harmonic response of blisk. Fig 17 shows the amplitude response of blade airfoil for 5% stimulus. Maximum amplitude of vibration is found at 688Hz.

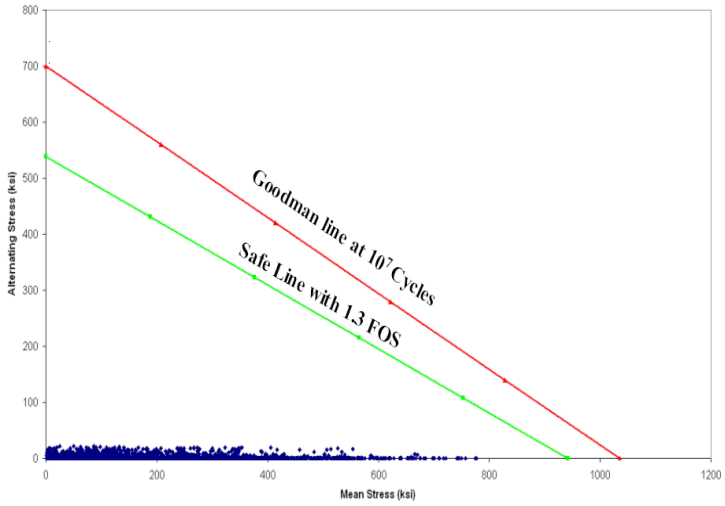

Fig 17: Goodman diagram for evaluation of vibratory stress margin

Subsequent peaks are found at other natural frequencies of the assembly. The stress evaluation is carried out at amplitudes varying from maximum to minimum. Maximum peak stress is found to be 53MPa for mode three frequencies, where possibility of resonance is predicted from interference diagram. The stresses obtained from harmonic analysis are used with static stress analysis to plot Goodman diagram for mode2 family (Fig5.13).For a mean stress of 790 MPa (static analysis) allowable alternating stress from good man diagram is 110MPa at Factor of safety line. From Goodman diagram it appears that a peak alternating stress of 53MPa can sustain 107 cycles at resonant frequency. Reasonable margin of safety for alternating stress indicates longer life of the component.

A very basic discussion on modal analysis is presented based on the principles of cyclic symmetry outlining the emphasis on cyclic symmetric modal analysis. Concept of nodal diameter was discussed to give an insight to the possible disk modes which occur during in-service life. Evaluation of resonance condition for a typical gas turbine bladed disk and blisk is discussed considering safety margins for the possible uncertainties due to manufacturing, temperature and stiffness variation due to spin softening and stress stiffening in blades. Various sources of excitations which disturb the blades in a gas turbine are outlined. Some aspects of cyclic symmetric modal analysis in ANSYS are discussed. Reason for pairing of natural frequencies is explained. SAFE diagram is discussed and its use in risk evaluation due to resonance is presented.

Table:5: Frequencies of the first 6 modes at different nodal diameter of Blisk

Nodal Dia	Mode1	Mode2	Mode3	Mode4	Mode5	Mode6
0	900	1472	2424	3227	3243	4122
1	894	1442	2425	2784	3389	3463
2	882	1384	2266	2434	3394	4061
3	899	1532	2433	3062	3515	4995
4	924	1880	2438	3384	4651	5976
5	938	2292	2455	3424	5844	6194
6	946	2427	2727	3460	6044	7068
7	950	2434	3045	3525	6071	7596
8	953	2437	3232	3669	6090	7754
9	955	2439	3305	3875	6107	7831
10	956	2441	3334	4081	6126	7885
11	958	2443	3347	4264	6145	7930
12	958	2444	3354	4419	6164	7967
13	959	2445	3359	4548	6183	7999
14	960	2446	3361	4654	6201	8026
15	960	2447	3363	4738	6218	8048
16	961	2448	3364	4803	6233	8066
17	961	2449	3364	4852	6245	8080
18	961	2449	3364	4885	6253	8089
19	961	2449	3365	4905	6259	8095
20	961	2449	3365	4911	6261	8097

CONCLUSIONS

Finite element investigation has been carried out to examine the influence of static stresses, vibrations, fatigue, over speed and burst margins limits on bladed disk and blisk. Typical trends and operating conditions of first stage compressor of a gas turbine engine are considered as encountered by them in practice. Analysis is carried out on 3D geometric models, considering model material as Ti-6Al-4V alloy typically employed to manufacture these components. The actual properties / characteristics obtained from valued published information's have been used as inputs to carry out various analysis employing ANSYS. In this respect, the objectives and goals set forth in this work have been satisfactorily achieved. The salient results of the investigations are summarized below.

Bladed disk

- Pre-stressing effects have captured the increased stiffness of the assembly and its effects on the frequency which increases linearly with speed.
- The fundamental cantilever mode is free from resonance with desired frequency margins in operating range.
- Predictions show higher modes have low frequency margins and are almost resonant.
- Evaluation of vibratory stresses employing Goodman criteria and stimulus approach at resonance points reveal the integrity of blades to achieve 1e8 cycles.

Blisk

- The blisk, weighing 8.92kg, has higher frequencies for the entire mode shapes with crossing over for fundamental cantilever mode occurring between three and four per rev in comparison with bladed disk assembly between two and three per rev.
- The fundamental cantilever mode is free from resonance with desired frequency margins at operating range.
- Disk participation is significant in the case of blisk, due to the thin web.
- Predictions show higher modes have low frequency margins and are almost resonant.
- Evaluation of vibratory stresses employing Goodman criteria and stimulus approach at resonance points reveal the integrity of blades to achieve 1e8 cycles.

Above study on structural evaluation of bladed disk and blisk for given operating conditions reveals blisk, can be a substitute to bladed disk with considerable gain up to 30% in weight reduction.

- Optimized blisk qualifies the tests on over speed and burst margin limits as per initial design requirement.
- Similar trends are noticed for static stresses and displacements to achieve satisfactory results for low cycle fatigue life.
- Desired frequency margins are achieved to promote blisk as a replacement to bladed disk. Subsequently, Goodman diagram provides reasonable margins for vibratory modes indicating safety of blades due to high cycle fatigue.

The present study on structural evaluation of bladed disk and blisk for given operating conditions reveals that the optimized blisk can be a substitute to bladed disk with considerable (30%) reduction in weight. Optimized blisk qualifies the tests on over speed and burst margin limits as per initial design requirement. Similar trends are noticed for static stresses and displacements to achieve satisfactory results for low cycle fatigue life. Desired frequency margins are achieved to promote blisk as a replacement to bladed disk. Subsequently, Goodman diagram shows reasonable margins for vibratory modes indicating safety of blades due to high cycle fatigue.

REFERENCES

1. E. Poursaeidi, M.R Mohammadi, Failure analysis of lock-pin in a gas turbine engine. Volume 15, Engineering Failure Analysis, Issue 7, October 2008, Pages 847-855.
2. R.I Jaffee, Titanium Steam Turbine Blading. 1st Edition Workshop Proceedings Palo Alto, California, 9-10 November 1988.
3. M. Janecek, F. Nový, P. Harcuba, J. Stráský, L. Trsko, M. Mhaede and L. Wagner, The very high cycle fatigue behaviour of Ti-6Al-4V alloy, Proceedings of the International Symposium on Physics of Materials (ISPMA13), Vol. 128 (2015).
4. T.Mekhail "Theoretical, Experimental and Numerical Investigation of the Effect of Blades Number on the Performance of the regenerative blowers"-IJCAS Vol.4 (2015)
5. T. Meakhail, and S. O. Park, An improved theory for regenerative pump performance, Proc. IMechE, Part A: J Power Energy, 2005, 219, 213-222.
6. M. Raheel, and A. Engeda, Current status, design and performance trends for the regenerative flow compressors and pumps, ASME International Mechanical Engineering Congress & Exposition, 17- 22, 2002.
7. Y. Senoo, A comparison of regenerative pumps theories supported by new performance data, Trans ASME, 1956; 78.
8. T. Meakhail, S. O. Park, D. Lee, and S. Mikhail, A Study of Circulating Flow in Regenerative Pump, Proceedings of the KSAS 1 st International Session, 2003, pp. 19–26.
9. H. W. Iversen, Berkeley, and Calif, Performance of the periphery pump, Trans ASME, January, 1955, 77.
10. M. Badami, Theoretical and experimental analysis of traditional and new periphery pumps, SAE Technical Paper Series, 1997, no. 971074, pp. 45–55.
11. G. Grabow, Influence of the number of vanes and vane angle on the suction behavior of regenerative pumps, Proceedings of Second Conference on Flow Machines, 1966, Budapest, pp. 147–166.
12. C. Jang, and J. Lee., Shape Optimization of a Regenerative Blower Used for Building Fuel Cell System, Open Journal of Fluid Dynamics, 2012, 2, 208-214.
13. Botag,.(2006).RetrievedApril4,2006,from https://commons.wikimedia.org/wiki/File:Lift_curve.svg.

